UDC 621.643.532.527.001.5
DOI: 10.15587/1729-4061.2017.108424

STUDY OF FUNCTIONING OF A VORTEX TUBE WITH A TWO-PHASE FLOW

V. Shaporev
Doctor of Technical Sciences, Professor*
E-mail: fiola2008@mail.ru
I. Pitak
PhD, Associate Professor*
E-mail: ipitak5@gmail.com
O. Pitak
PhD, Associate Professor
Department of Labour Protection and the Environmentl**
E-mail: okatip@rambler.ru
S. Briankin
Head of course
Faculty of military training**
E-mail: serzh2082@ukr.net
*Department of chemical technique and industrial ecology**
**National Technical University «Kharkiv Polytechnic Institute»
Kyrpychova str., 2, Kharkiv, Ukraine, 61002

Розглядається процес підготовки запиленого газового потоку з технологічного джерела перед подачею його в апарат-пиловловлювач з метою підвищення ефективності уловлювання пилу. Описано умови для деструкції шкідливих газових домішок і утилізації непридатного тепла очищеного газового потоку. Створена розрахункова математична модель для визначення поля швидкостей газодисперсного потоку в робочій порожнині вихрової труби. Встановлено, що нерівномірний розподіл швидкостей по радіусу забезпечує інтенсивну дисипацію механічної енергії, внутрішнє тепловиділення і нерівномірний розподіл температури гальмування

Ключові слова: суха очистка, пиловий потік, вихрова труба, ефект Ранка, гідродинаміка, ефективність пиловловлення, агломерація часток, математична модель

Рассматривается процесс подготовки запыленного газового потока из технологического источника перед подачей его в аппарат-пылеуловитель с целью повышения эффективности улавливания пыли. Описаны условия для деструкции вредных газовых примесей и утилизации бросового тепла очищенного газового потока. Создана расчетная математическая модель для определения поля скоростей газодисперсного потока в рабочей полости вихревой трубы. Установлено, что неравномерное распределение скоростей по радиусу обеспечивает интенсивную диссипацию механической энергии, внутреннее тепловыделение и неравномерное распределение температуры торможения

Ключевые слова: сухая очистка, пылевой поток, вихревая труба, эффект Ранка, гидродинамика, эффективность пылеулавливания, агломерация частиц, математическая модель

1. Introduction

As it is generally known, the main task at present of gas scrubbing is to bring content of toxic impurities in gas emissions to maximum permissible concentrations established by sanitary code. The methods used for the removal of aerosols (dust) and gaseous and vaporous impurities from gases vary depending on the nature of harmful impurities. All methods of gas scrubbing are determined primarily by physico-chemical properties of impurities, their aggregate state, dispersity, chemical composition, etc. The variety of harmful impurities in industrial gas emissions and their physico-chemical properties brings about a large number of cleaning methods, devices and reactors used.

The greatest success in the centrifugal capture of particulate dust from gas flows was observed in the field of hardware implementation rather than in scientific designs. This is due to the accumulation of a many years' experience in operation of industrial devices on the one hand and a high complexity of the gas-solid system in the centrifugal field on the other hand. The theory of operation of cyclones and other devices for dry cleaning of gas flows from dust has not yet been improved and does not provide the possibility for a reasonable choice of the device and its main characteristics. Therefore, study of flow conditions in the dry gas purification device, redistribution of energy under various conditions and influence of physical and chemical characteristics of the gas flow on these parameters is a relevant issue and will improve device efficiency.

2. Literature review and problem statement

The processes of cleaning technological and ventilation emissions taking place at chemical, processing, metallurgical, machine-building enterprises from gas, dust and vapor impurities are characterized in many cases by a number of features [1, 2]:

– gases emitted into atmosphere have a rather high temperature (especially after leaving furnaces, reactors) reaching at times 673÷873 K and contain large amounts of dust (more than 5 g/Nm^3) which significantly complicates the cleaning process and requires preliminary gas preparation;

– concentration of gaseous and vaporous impurities more often in ventilation and less often in the process emissions is variable and relatively low.

As a rule, NO_x, SO_x, CO, HCl, HF, SiF_4, NH_3 individually or in a combination, depending on the process type, are present as gaseous impurities in the gas stream. Concentration of each component can range from 50 to 100 mg/Nm^3. In many cases, the task set during gas purification is not just

to bring the content of harmful components to the maximum allowable concentrations in the emitted gases but also to use exhaust heat of the purified gas [3, 4]. In other cases, for example in production of soda ash [5], the purified gas leaving shaft furnaces and calciners should not contain more than 5 mg/m^3 of aerosol since it must be subjected to compression and then used in subsequent manufacturing operations. In industrial conditions, to achieve maximum allowable aerosol concentrations and eliminate gaseous impurities, combined methods are commonly used in the process of gas cleaning such as dry+wet gas cleaning [6, 7]. Disadvantages of such schemes are well known [8]: high (0.4÷4.2 kg/Nm^3) consumption of liquids (water) and formation of suspensions and slurries. Virtually no purification from such gaseous impurities as NO_x, SO_x, CO is ensured. The exhaust heat of gases is not used and installation of additional equipment is required for separation and filtration of slurry suspensions.

The first stage, dry gas cleaning, is carried out in widely used centrifugal-inertial devices, such as cyclones of various designs [9]. Cyclones are notable for high gas productivity, design simplicity and operational reliability. For example, for high-yield cyclones, in particular battery cyclones (with a productivity of more than 20,000 Nm^3/h), purification efficiency is 20–30 % for d=2÷5 μm average particle size; 40–60 % for d=5÷20 μm and 90–92 % for d>30 μm [10].

Resistance of a high-performance cyclone is about 1080 Pa. Obviously, cyclones work most effectively if the particle size is d>30 μm. This conclusion is valid even for the most effective TsN-11 cyclone [11]. Therefore, many current studies are aimed at improvement of the centrifugal-inertial cleaning of gas flows and corresponding device designs [12–14]. All improvements in the devices can be classified according to the following characteristics:

– a tube or a branch tube at the entry of dusty gas stream to the main unit;

– a main unit where separation takes place;

– an outlet branch tube for the purified gas stream and a hopper and an outlet branch tube for the trapped dust.

Hence, it is advisable to consider such an option that when a dusty gas stream is fed into the main unit like a setting forebunker for dry scrubbing, preparation of the gas before its coming to the forebunker could be carried out in vortex tubes with a partial recirculation of the heated gas due to the Ranque effect. Principal provisions of such an approach were discussed in [15–17] where it was noted that implementation of the 'vortex tube – setting forebunker' scheme can ensure fine cleaning of the incoming gas from impurities and utilization of the purified gas energy. However, there are no experimental data that would confirm the above conclusion for specific industrial conditions [15–17]. Besides, there is no mathematical description of the processes taking place in the vortex tube and in the forebunker for these conditions.

Obviously, the process in the vortex tube can be regarded as a gas-phase chemical process proceeding under non-isothermal conditions. To control this process, it is necessary to clarify the effect of changes in the initial conditions (temperature, concentration ratio, nature of the particle size variation, hydrodynamic conditions) and solve a system of differential equations constituting a mathematical model of the process. The basic choice is the choice of the vortex tube design, i. e. the ratio of dimensions, the tube cross-sectional profile (tapering, presence of bends, etc.) which provides one or another hydrodynamic situation affecting distribution of temperatures, concentrations, and other parameters. The vortex tube under these conditions can be considered as a process control object. As is known, to describe the control object, it is necessary to establish connections between its inputs and outputs taking into account the model of the medium flow in the vortex tube. Therefore, the first part of the studies is based on the fundamental concepts of flow of swirled streams [13–17, 18–20] and on the analysis of known experimental data concerning flow of a swirling stream in a vortex tube [21–24] and is devoted to a mathematical description of a reaction medium motion in the vortex tube.

3. The study objective and tasks

The study objective was to make a mathematical description of flow of aerosol-containing manufacturing waste gases in a vortex tube under the conditions ensuring occurrence of the Ranque effect and analyze "physics" of the processes taking place in the model for various process parameters of the gas flow at the inlet to the vortex tube.

To achieve this objective, the following tasks were set:

– to analyze physico-chemical characteristics of manufacturing and ventilation emissions at enterprises and establish characteristic indicators for dust (fractional composition, temperature of gas-dust flows);

– to study the mathematical model of a gas-dust stream flow in a vortex tube (determine velocity fields, trajectory of movement of dust particles and analyze temperature distribution in the stream);

– based on the developed mathematical model of the gas-dust flow in a vortex tube, to analyze the possibility of aggregation of dust particles and destruction of NO_x, SO_x, CO gas impurities.

4. Study of the process of cleaning the gas-dust stream

A schematic diagram of the vortex tube is shown in Fig. 1 [25].

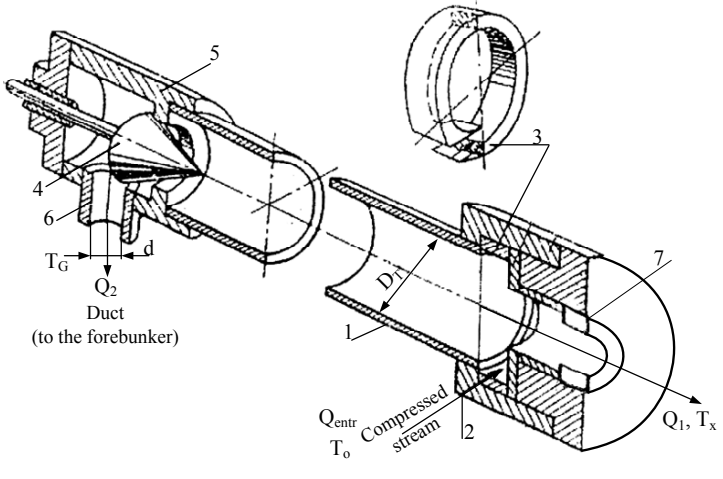

Fig. 1. Schematic diagram of the vortex tube: reaction tube (1); nozzle (connecting tube) for supply of compressed gas from the process source (2); gas swirler (3); control valve (4); gas outlet chamber (5); connecting tube for supply of the compressed gas to the forebunker (6); diaphragm (7)

The vortex tube (Fig. 2) usually has a cylindrical body 1 with a diaphragm 2 inside. A nozzle is located tangentially beside it. A throttle valve 4 is located at the opposite (hot) end of the tube.

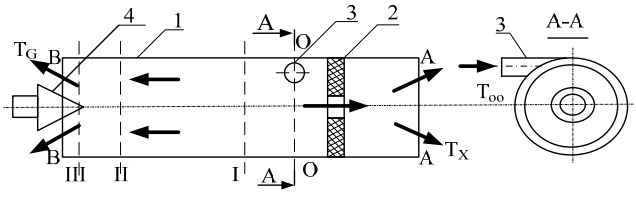

Fig. 2. Schematic view of the vortex tube: tube (1); diaphragm (2); nozzle (3); valve (4)

Compressed air (gas) enters the nozzle 3. When tangential stream of air enters the tube 1, it swirls forming a rotating stream inside the tube and acquiring kinetic energy. The air moves in a vortex stream with different angular velocities. The rotation speed at the tube axis is higher than at the periphery. Therefore, having given their kinetic energy to the inner layers of air, the outer layers cool down to a temperature T_x and exit through the diaphragm 2. The air heated to temperatures T_r exits thru the free end of the tube. Flow and temperature of the air are regulated by the throttle valve 4. Temperature of the cooled air depends on its initial parameters, i.e. pressure and temperature as well as on the device design.

Symbols O, I, II, III, A, B in Fig. 2 denote the conditional sections of the vortex tube at which dynamic structure of the flow and loss of kinetic energy are considered. At one end (A-A section), flow exits through the aperture (diaphragm) in the axis of the tube. At the opposite end of the tube, there is an outlet in a form of a peripheral annular gap (B-B section). As experience shows, with an adiabatic flow of a viscous gas in the tube, the gas flowing through the central hole in A-A section has much lower braking temperature than at the periphery (B-B section). For example, according to experimental data, maximum difference in braking temperatures corresponding to section I-I reaches a value of $T_{oo}-T_o=80-90$ °C. With movement away from O-O section, the profile of braking temperatures is equalized and the temperature difference reaches 40 °C at section III. Braking temperature T_o at the tube periphery varies along the tube less intensively than at its axis where it increases sharply towards B-B section. The lowest braking temperature on the axis corresponds to I-I section. Thus, it is obvious that temperature distribution in the gas flow takes place in the vortex tube and the cooled gas exits thru the central hole (A-A section).

Efficiency of temperature separation in the gas flow is practically independent of the initial gas temperature T_{oo}, it depends weakly on P_x/P_{oo} ratio and is lower the higher initial pressure P_o. However, efficiency depends on the Rossby number, R_o, which is a measure of ratio of the momentum in the axial direction to the angular momentum $R_o=QL/r_{oo}R$. Here Q is the volume flow in the axial section, L is the tube length connecting "n" calibers of its radius (R), $r_{oo}=2\pi C_{\theta R}R$ is the circulation on the bounded surface, R. Development of the swirling flow in the channel occurs under the continuous action of viscous shear stresses in the boundary layers on the walls (or in the vicinity of the axis). This effect leads to a complete decay of rotation, the faster (in a smaller section of the channel length) the larger the Rossby number. Next, a normal parabolic profile of the axial velocity is established. The process of development of such a steady profile is lengthened by swirling of the flow. Thus, at the point (zone) of transition to a parabolic profile of the axial velocity, $d\varphi/dz\rightarrow 0$, that is, the component of angular velocity of the particle (the terms characterizing the vortex motion of the stream) and their z derivative tend to zero. The structure of flow in the vortex tube is complicated. In the near-axis area, there is a flow exiting through the throttle. In this case, the return flow through the diaphragm can be considered forced and its intensity depends on the state of the passage areas of the throttle and the diaphragm. When the diaphragm is closed, a return flow characteristic of the swirling flows in common appears at sufficiently high velocities near the flow axis. Thus, two forms of swirling flow are observed inside the vortex tube when the circumferential velocity profile in the return flow zone (I→O→A sections) is close to a quasi-solid type of rotation and close to a quasipotential type of rotation in the peripheral zone (II→III→B sections). Therefore, analysis and calculation of the process are based on a simplified scheme of flow dynamics and an energy equation.

A homogeneous gas is fed to the zero section of the vortex tube under P_{oo} pressure (most often, studies are carried out for air). As noted above, the gas system to be treated in the vortex tube may contain various gas components in various proportions (for example, H_2O, CO_2, H_2, N_2, O_2) and in addition, the above toxic gas impurities and aerosols (up to 10 g/Nm^3) with various particle sizes. At the same time, the gas at a flow rate of 1000÷15,000 Nm^3/h, (0.3÷4.2 Nm^3/s) having temperature of 673–873 K enters the vortex tube under pressure (1.5÷2.5 atm). Taking into account that the internal diameters of the vortex tubes for these gas flow rates are within ($5\cdot10^{-2}\div25.0\cdot10^{-2}$ m) [15–17], the flow velocity can reach 80÷100 m/s at the inlet.

The characteristic of the described gas mixture will influence the process in the vortex tube due to the change in viscosity, density, concentration, particle size, chemical composition and specific surface area. Chemical interactions between the medium components are possible. Influence of some of these parameters on the process in the vortex chambers is described in literature. For example, works [25, 26] studied technological processes and devices in which baking of raw materials, drying and dry hydration of the baked products are fundamental. The aim was to determine chemical composition and dispersity of aerosols in exhaust gases. The results of the studies are presented in a form of nomogram (Fig. 3).

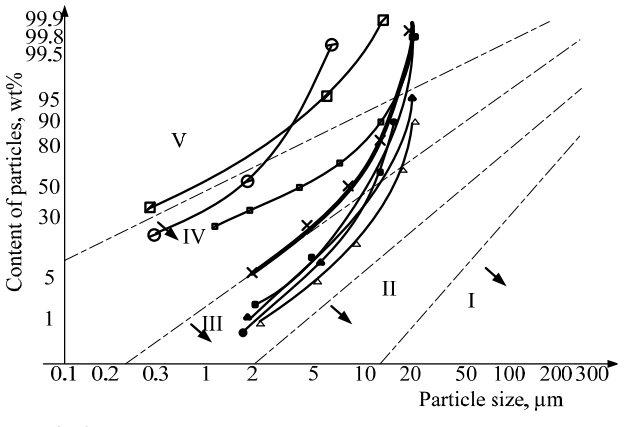

Fig. 3. Classification nomogram for determining dust group: ⊖ – for magnesium oxide (firing $MgCO_3\cdot H_2O$); ⧄ – for ZnO (production of dry zinc white); ◘ – for hydrate of lime; ✕ for lime; ■ – for barium carbonate; ▲ – for sodium bicarbonate; ● – for soda ash; △ – for washing powders

It gets obvious from Fig. 3 that according to the classification, overwhelming majority of aerosols in exhaust gases belong to the class of fine and very fine dusts which are practically not captured by cyclones. Besides that, dust particles, such as CaO, MgO, Ca $(OH)_2$, ZnO have a sufficiently large specific surface (according to BET method, up to 10 m^2/g) which indicates their sufficiently high adsorption capacity, e. g. with gas impurities, and aggregation capability. Analysis of the obtained data also showed that the particle size distribution in these aerosols obeys multimodal distributions, $f(x)$, of the following form:

$$f(x)=\frac{W\left(x-x_{\min 1}\right)^{a_1 m_1}\left(x_{\max 1}-x\right)^{m_1}}{\int\limits_{x_{\min 1}}^{x_{\max 1}}\left(x-x_{\min 1}\right)^{a_1 m_1}\left(x_{\max 1}-x\right)^{m_1}\mathrm{d}x}+$$
$$+\frac{(1-W)\left(x-x_{\min 2}\right)^{a_2 m_2}\left(x_{\max 2}-x\right)^{m_2}}{\int\limits_{x_{\min 2}}^{x_{\max 2}}\left(x-x_{\min 2}\right)^{a_2 m_2}\left(x_{\max 2}-x\right)^{m_2}\mathrm{d}x}, \quad (1)$$

where W is the mass fraction of fine particles; $(1-W)$ is the mass concentration of the coarse fraction; x is the absolute size, $x_{\min}$, $x_{\max}$ are the smallest and the largest absolute sizes.

This type of function makes it possible to track changes in the particle size during processing more accurately and with higher probability. In [27, 28], a possibility of aggregation of dust particles with characteristics close to those shown in Fig. 3, under hydrodynamic conditions corresponding to the I-I section, i. e., to the quasi-solid type of rotation of the gas flow, has been established theoretically and experimentally. It was shown that the amount of a very fine fraction (particle size less than 5 μm) decreases in 2–2.5 times due to aggregation of particles. It was established in [29] that aggregation of dust particles occurs even more intensively under the action of the alternating longitudinal pressure gradient that arises in the tube when the gas flow moves to the B-B section due to alternate convergent and divergent sections. Such flows are realized in undulating channels and the vorticity transfer equation for this case, as it was established by the researchers, can be written in a following form:

$$\frac{\partial\zeta}{\partial\theta}+\frac{\mathrm{Re}}{A^{x_2}}\left(U\frac{\partial\zeta}{\partial x}+V\frac{\partial\zeta}{\partial x}\right)=\frac{1}{A^{x_2}}\nabla^2\zeta. \quad (2)$$

The relationship between vorticity and the stream function:

$$\zeta=-\nabla^2\varphi, \quad (3)$$

where ζ is dimensionless vorticity; θ is dimensionless time; Re is Reynolds number $\mathrm{Re}=\overline{Q}/\nu$; $\overline{Q}$ is time-averaged flow rate per channel diameter unit area, m^2/s; ν is kinematic viscosity, m^2/s; $A^x=H_{\max}\sqrt{\frac{\omega}{\nu}}$; $H_{\max}$ is maximum distance between the wave walls, m; ω is the angular frequency, 1/s; U, Y are dimensionless velocities in the X direction (along the channel) and in the Y direction (the channel radius), respectively; φ is dimensionless stream function.

It was suggested in [30] to determine vorticity near the wall as follows:

$$\zeta_W=\overline{\zeta_W}+\sum_{i=1}\Phi_i\sin(\theta+\Phi^{'}_i), \quad (4)$$

where Φ_i is amplitude of vorticity oscillation near the wall at the i-th oscillation (narrowing – expansion); $\overline{\zeta_W}$ is dimensionless instantaneous vorticity at the wall; $\Phi^{'}_i$ is vorticity phase difference at the wall with respect to the flow at the i-th oscillation.

Analysis of equations (2)–(4) as well as the data given in work [31] where effect of the nature of aerosol flow rotation during movement in the tube on stratification of aerosols was studied has established that the flow downstream the mixing zone is close to the quasi-potential flow. The nature of stratification of particles does not depend on the curvature of the channel but rather on the tangential velocity of the aerosol in the circumferential direction; it also shows a similar motion of pure and dusty gases.

Thus, it can be assumed that hydrodynamics and nature of motion of the dust stream in the vortex tube will be the same as for a pure gas. The content of suspended matter (dust) in the gas stream up to 10 g/Nm^3 which changes the level of velocities does not affect the character of their distribution, and the change in the tangential velocity profile practically does not affect the trajectory of the aerosol particles if the average level of velocities remains constant [32, 33]. A possibility of a physico-chemical transformation of gaseous impurities (NO_x, CO, SO_x) in excess of H_2O vapors relative to the mass of impurities was considered for a combustible swirling stream moving in a vortex tube [34, 35]. The excess of H_2O vapors is maintained within the following limits: H_2O vapor mass, mg/gas impurities mass, mg=5÷10. A homogeneous catalysis of the following type takes place in a stream:

$$CO + H_2O \rightarrow CO_2 + H_2,$$
$$2H_2 + O_2 \rightarrow 2H_2O, \quad (5)$$

at stream temperatures of 673÷873 K.

The rate of chemical transformation was considered as a function of intensity of the heat and mass transfer processes in a stream. The resulting rate of chemical reaction "W" for one component was determined as:

$$W=W_r/K_o, \quad (6)$$

where W_r is the rate of the direct reaction; $1/K_o=1-P_a$ where

$$P_a=\frac{k_2/k_1}{a^{\alpha}b^{\beta}/\left(m^{\mu}n^{\eta}\right)},$$

a, b are concentrations of gas impurities; μ, η, α, β are stoichiometric coefficients; P_a is the criterion of equilibrium; K_o is criterion of contact, $K_o=\left(k_1a^{\alpha}b^{\beta}\right)/\left(\partial C/\partial\tau\right)$; C is concentration of initial substances; k_1, k_2 are constants of the direct and reverse reaction rates.

In a general case, the process kinetics is completely determined by the conditions of mass and energy transfer:

$$P_a=f\left(\mathrm{Re},\mathrm{Pr_T},\mathrm{Pr_D}\ldots\right), \quad (7)$$

where $\mathrm{Pr}_T=\nu/\alpha$ is the Prandtl criterion for heat exchange; α is coefficient of temperature conductivity; $Pr_D=\nu/D_c$ is Prandtl's criterion for material exchange; D_c is the diffusion coefficient of gas impurities; v is coefficient of kinematic viscosity, m^2/s.

The results of experimental studies have shown that concentration of gaseous toxicants under the abovementioned

conditions can be reduced by a factor of 2–3. This result correlates with the data of industrial tests of reduction of NO_x oxides concentration in the exhaust of gas turbine installations due to injection of steam into the combustion chamber [36]. Analysis of the data showed that all considered positive effects which were observed in purification of exhaust gases in the vortex tubes are explained by certain conditions of viscous gas turbulent flow. This occurs in three main sections (areas), namely (O→I, I→II→III, O→A), and accordingly at a quantitative ratio of flow rates. When creating a computational mathematical model for determining velocity field in the working cavity of the vortex tube, it is necessary to take into account not only conditions for formation of flows in the device but also conditions of aerodynamic situation that leads to the Ranque effect. To create the model, use the schematic calculation diagram of the vortex tube which provides for aerosol separation, Fig. 4.

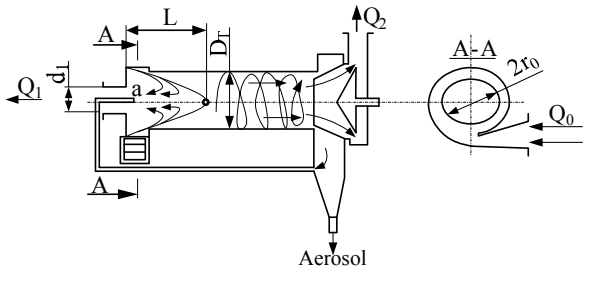

Fig. 4. Schematic view of a vortex tube with a snail swirler: *Do* is the device diameter, m; d_1 is diameter of diaphragm opening, m; Q_o is total flow rate of the working substance, m^3/h; Q_1 is flow rate of the cooled stream, m^3/h; Q_2 is flow rate of the heated flux, m^3/h; L is the length of the energy separation section of the working substance, m

Assume that the flow regime of the gas stream in the device is turbulent and the working substance is a viscous, compressible gas. The stream is strongly turbulized in the zone of energy separation and the self-similarity of the process is observed according to the Re number ($Re>10^5$), therefore, Re is taken constant in the calculations. With a greater degree of probability, steady-state heat and mass transfer in the asymmetric flow of a vortex stream can occur throughout the region at a constant Pr number value of Pr<1 (Pr≈0.64÷0.7). The walls of the tube are considered to be insulated, so there is no heat exchange between the gas and the external medium. The effect of the Re number on the turbulent layer (flux) at high velocities downstream the swirler in I–III and O-A zones (Fig. 1, 2) is the same as the effect on the flow of incompressible substance [18–20] and therefore it can be assumed that the gas flow is potentially circulating, that is, the particles (the gas moles) rotate around a certain axis that does not intersect the trajectories but do not rotate relative to their own axes, and therefore ω=0. In the O-I region (Fig. 1, 2), at a "quasi-solid" motion of the rotating flow with $Re\geq10^5$, Taylor vortices and toroidal Hill vortices are formed. In this case, tangential components of velocity of the gas volumes moving towards the center and periphery are arbitrarily set relative to the radius. The turbulent flow of a viscous gas in the region of the swirler causes flow rearrangement and ensures a situation of gas-dynamical energy separation provided that the number Re of the flow (Q_o) is $Re\geq10^5$ at the inlet. At the same time, the non-uniform distribution of velocities along the radius explains the intensive dissipation of mechanical energy, internal heat release and uneven braking temperature distribution. Therefore, the length of the vortex zone (L) and the velocity distribution in it are of decisive importance for the processes occurring in the gas flow and for the vortex tube calculation.

Thus, the pattern of flows will take the following form. A circular source of quasi-solid rotational flow (Q_o flow) is formed at the periphery of the swirler (Fig. 1), near the wall where the diaphragm is located. In the center of the diaphragm, there is a drain (Q_1 flow rate) at the device axis with a capacity equal to the flow rate of the cooled gas. The difference in the flow rates of the working medium between the ring source and the central run-off of the cooled gas (Q_o-Q_1) is the flow rate Q_g of the heated (hot) gas.

The axisymmetric motion with rotation of the ring source is described in [18–20] by a system of Navier-Stokes equations and the continuity of energies and states using an empirical relationship between viscosity coefficients and temperature.

The equation of continuity:

$$\frac{\partial(r\rho c_r)}{\partial r}+\frac{\partial(\rho c_z)}{\partial z}=0. \tag{8}$$

Navier-Stokes equation:

$$\rho\left(c_r\frac{\partial c_r}{\partial r}+c_z\frac{\partial c_r}{\partial z}-\frac{c_\theta^2}{r}\right)=\frac{\partial\rho}{\partial r}+\frac{2}{r}\cdot\frac{\partial}{\partial r}\left(\mu r\frac{\partial c_r}{\partial r}\right)-$$
$$-\frac{2}{3}\cdot\frac{\partial}{\partial r}\left(\mu\overline{div c}\right)+\frac{\partial}{\partial r}\mu\left(\frac{\partial c_z}{\partial r}+\frac{\partial c_r}{\partial z}\right)-\frac{2\mu}{r}\cdot\left(\frac{c_r}{r}\right),$$

$$\rho\left(c_r\frac{\partial c_z}{\partial r}+c_z\frac{\partial c_z}{\partial z}\right)=-\frac{\partial p}{\partial z}+\frac{1}{r}\cdot\frac{\partial}{\partial r}-$$
$$-r\mu\left(\frac{\partial c_z}{\partial r}+\frac{\partial c_r}{\partial z}\right)+\frac{\partial}{\partial z}\left(2\mu\frac{\partial c_z}{\partial z}-\frac{2}{3}\mu\overline{div c}\right). \tag{9}$$

$$\rho\left(c_r\frac{\partial c_\theta}{\partial r}+c_z\frac{\partial c_\theta}{\partial z}+\frac{c_r c_\theta}{r}\right)=$$
$$=\frac{1}{r^2}\cdot\frac{\partial}{\partial r}\left[r^2\mu\left(\frac{\partial c_\theta}{\partial r}-\frac{c_\theta}{r}\right)\right]+\frac{\partial}{\partial z}\cdot\mu\frac{\partial c_\theta}{\partial z}.$$

Equation of energy:

$$\frac{1}{r^2}\cdot\frac{\partial}{\partial r}\left\{r\left[\rho c_r\left(i+\frac{c^2}{2}\right)-\mu\frac{\partial\left(\frac{i}{\mathrm{Pr}}\right)}{\partial r}-2\mu c_r\frac{\partial c_r}{\partial r}-\mu c_\theta\left(\frac{\partial c_\theta}{\partial r}-\frac{c_\theta}{r}\right)-\mu c_z\left(\frac{\partial c_z}{\partial r}+\frac{\partial c_r}{\partial z}\right)+\frac{2}{3}\mu c_r\overline{div c}\right]\right\}+$$
$$+\frac{\partial}{\partial z}\left[\rho cz\left(i+\frac{c^2}{2}\right)-\mu\frac{\partial\left(\frac{i}{\mathrm{Pr}}\right)}{\partial z}-\mu c_r\left(\frac{\partial c_z}{\partial z}+\frac{\partial c_r}{\partial z}\right)-\mu c_\theta\frac{\partial c_\theta}{\partial z}-\mu c_z\frac{\partial c_z}{\partial z}+\frac{2}{3}\mu c_z\overline{div c}\right]=0. \tag{10}$$

The system end equations:

$$\frac{P}{\rho}=R^*T,\quad\frac{\mu}{\mu_0}=\left(\frac{T}{T_0}\right)^{1,5}\frac{T_0+T_s}{T+T_s}, \tag{11}$$

where r, θ, z is cylindrical coordinate system; C_r, C_θ, C_z are the velocity components; ρ is medium density; μ is medium viscosity; T is medium temperature, K; R^* is universal gas constant; i is enthalpy; z axis is along the channel axis; r axis is normal to z axis.

The condition of axial symmetry implies absence of gradients in the circumferential direction.

To connect the tensor of turbulent directions with the averaged values of velocities, use the Prandtl hypothesis (the semi-empirical theory of the mixing length).

Then the relationship between the turbulent stress tensor and certain velocities will be written by a system of equations:

$$\left.\begin{aligned}
&-\overline{\rho C_r^{12}}=2A\frac{\partial C_r}{\partial r};\ -\overline{\rho C_r' C_0'}=A\left(\frac{1}{r}\frac{\partial C_r}{\partial r}+\frac{\partial C_z}{\partial z}\right);\\
&-\overline{\rho C_0^{12}}=2A\left(\frac{1}{r}\frac{\partial C_0}{\partial z}-\frac{C_r}{r}\right);\ -\overline{\rho C_r' C_z'}=A\left(\frac{\partial C_r}{\partial z}+\frac{\partial C_0}{\partial r}-\frac{C_0}{r}\right);\\
&-\overline{\rho C_z^{12}}=2A\frac{\partial C_z}{\partial z};\ -\overline{\rho C_0' C_z'}=A\left(\frac{\partial C_r}{\partial z}+\frac{1}{r}\frac{\partial C_z}{\partial z}\right),
\end{aligned}\right\} \qquad (12)$$

where A is the coefficient of turbulent viscosity.

Taking into account that the coefficient of turbulent viscosity is a linear function of radius, that is, it increases from the center of the tube to its periphery (wall), then the boundary conditions for solving the systems of equations (8)–(12) will be as follows:

$$C_r=0; C_\theta=\omega(r)r; C_\theta=0; P=P_0 \quad \text{at } z=0,$$

$$C_r=0; C_\theta=0; C_z=\text{const}; P=\text{const} \quad \text{at } z\to\infty, \qquad (13)$$

where P is the pressure of the carrier medium, Pa; ω is the angular velocity of the flow rotation downstream the swirler, rad/s.

For the above parameters of the input stream, the system of equations (8)–(12) was computed using the method of finite differences with replacement of the first derivatives with the left differences, and the second derivatives with the right differences. The resulting system of equations with respect to the value of the unknown functions at the grid nodes was solved by the method of coordinate descent.

As a result, the components of the velocity of the first flow (O-I) can be determined from the expressions:

$$C_r=r\omega F_1(z);\ \ C_\theta=r\omega F_2(z);$$

$$C_z=\sqrt{B\omega}\cdot F_3(z), \qquad (14)$$

where $B=(1+A/\mu)\nu$; μ is coefficient of dynamic viscosity ns/m^2; v is coefficient of kinematic viscosity m^2/s.

In this case, in accordance with [18–20], the following quantity is considered as the parameter of flow twist:

$$\Lambda_\theta=\sqrt{\frac{K-1}{2}}\cdot\zeta_0, \qquad (15)$$

where K is the index of the gas property, $\zeta_0=\frac{C_0}{a_0}$; $a_0=\sqrt{(K-1)\cdot i_0}$ is velocity of sound in the state of braking; i_0 is the specific enthalpy of the moving gas.

The values of the calculation functions F_1, F_2, F_3, dimensionless velocity components, are shown in Fig. 5.

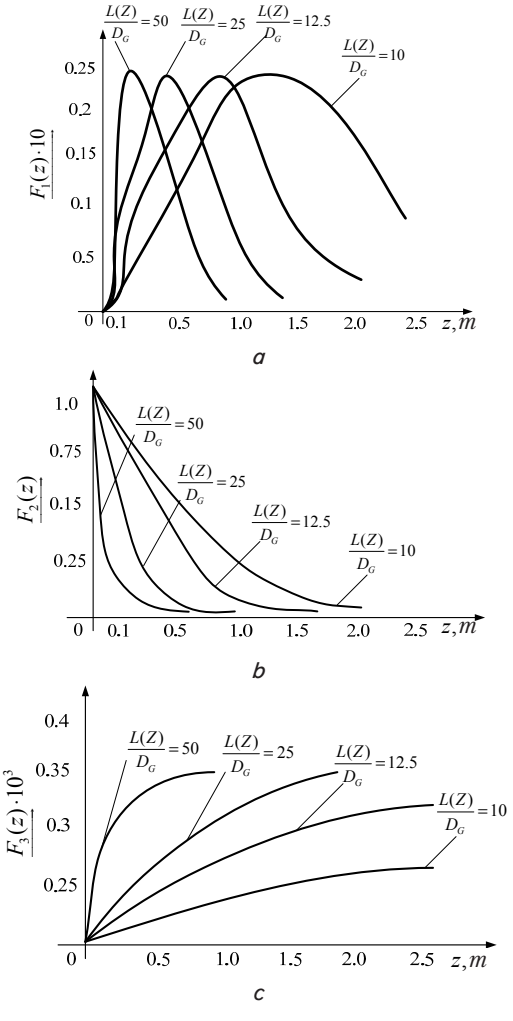

Fig. 5. Distribution of functions $F_1(z)$, $F_2(z)$, $F_3(z)$ along the length of the vortex zone: $F_1(z)$ function (*a*); $F_2(z)$ function (*b*); $F_3(z)$ function (*c*)

Parameter (15) characterizing intensity of flow swirling at each radius in the initial section is explicitly related to the degree of expansion of the working substance in the device. The calculations were carried out for various $L(z)/D_T$ ratios and the values of 0.05; 0.1; 0.2; 0.25 m were considered as D_T. We admit that the swirlers had diameters analogous to the D_T dimension and the width of rings was 0.014 m in all cases. Each ring had 8 tangential $0.1\cdot10^{-2}$ m wide, $1\cdot10^{-2}$ m high slots with 16 tangential 0.003 m diameter round holes and tangential 8 $0.3\cdot10^{-2}$ m diameter supersonic nozzles. The slots and holes were evenly distributed around the swirler perimeter.

It was also assumed that the area of the annular slot at the B-B section was at least 10 times larger than the total area of the entry slots of the swirler. Thus, at a steady flow rate Q_0, parameter (15) changed as a function of D_T due to a change in the linear velocity of the gas flow ahead of the swirler inlet. This velocity varied from 50 to 150 m/s for the abovementioned mass flows.

Analysis of the obtained dependences (graphs) in Fig. 5 allows us to conclude that intensity of motion of the gas flows changes significantly along the tube length and it was observed that rotation along the device was damping with the growth of the distance from the swirler. The tangential velocity component C_θ (function $F(z)_2$) is significantly reduced along the pipe length. The higher intensity of the

working substance twist, the more pronounced is the law of the flow velocity decrease along the zone length (Fig. 5). The nature of this decrease is similar for any value of D_T and its intensity depends on the law of distribution of the angular velocities along the radius in the initial section and is specified by parameters of the working substance, the twist parameter and the tube geometry. It is characteristic that the axial components of velocity in the section under consideration (Fig. 5) are directed from the mixing zone toward the diaphragm, that is against the motion of the hot stream. The numerical value of $F(z)_3$ is small but, nevertheless, this indicates appearance of reverse currents. As can be seen from Fig. 5 ($F(z)_3$; $F(z)_1$), the reverse flow exists in a zone close to the vortex chamber. Apparently, the vortex chamber has an annular shape. Further, when the flow moves to the B-B section, distribution of C_θ becomes different, the zone of quasi-solid rotation reduces, the absolute value of C_θ decreases due to friction of the gas flow against the wall and internal friction between the gas layers and the boundary layer grows. Apparently, the bulk of the aerosol moves in the boundary layer or a layer close to it. This aerosol aggregates (coagulates) in the zone of quasi-solid rotation where maximum values of C_r are attained (Fig. 5) as shown in [27, 28]. Motion of a dispersed phase in the vortex tube is determined by integrating the dynamic equations:

$$\frac{dz}{d\tau}=\upsilon_z;\ \ m\frac{d\upsilon_z}{d\tau}=F_z,$$

$$\frac{dr}{d\tau}=\upsilon_r;\ \ m\frac{d\upsilon_r}{d\tau}=F_r+m\frac{\upsilon_\tau}{r}, \qquad (16)$$

$$\frac{d\varphi}{d\tau}=\frac{\upsilon_\tau}{r};\ \ m\frac{d\upsilon_\tau}{d\tau}=F_\tau,$$

where z, r, φ are cylindrical coordinates of the particle; υ_z, υ_r, υ_τ are components of the particle velocity vector; F_z, F_r, F_τ are components of the vector of the force acting on the particle from the gas side; τ is time; m=ρ ($\pi d^3/6$) is the particle mass; ρ is the aerosol material density; d is the aerosol particle diameter.

To find the force F vector, use the following expression:

$$\vec{F}=\theta\rho_T\frac{\pi d^2}{4}\frac{\left|\overline{W}-\vec{\upsilon}\right|\left(\overline{W}-\vec{\upsilon}\right)}{2}-\frac{\pi d^3}{6}\nabla P, \qquad (17)$$

where θ is the coefficient of aerodynamic resistance,

$$\theta=\frac{24}{\mathrm{Re}}\left(1+\frac{\mathrm{Re}^{2/3}}{6}\right);\ \ \mathrm{Re}=\left(\left|W-\upsilon\right|\cdot d\right)/\nu;$$

ν is kinematic gas viscosity; ρ_Γ is the gas density; $\overline{W}(z,r,\varphi)$ is the gas velocity field; $P(z,r,\varphi)$ is the field of gas pressures.

The system of equations (16) was solved numerically using the Runge-Kutta method for the following initial conditions: τ=0; z=0; r=r_0; φ=0; υ_z=0; υ_r=0; υ_r=0.9 W(0; r_0; 0).

The calculated trajectories of motion of the aerosol particles which have entered the volume of the vortex zone at various radii, are presented in Fig. 6.

As can be seen from Fig. 6, the aerosol particles rapidly gain tangential and radial velocity and run under the action of inertial forces along a spiral path to the device periphery (towards the cylinder walls and the B-B section) regardless of the working zone radius. It should be noted that trajectories of the particles correlate with the trajectory of a change in the function $F_{1(z)}$ (Fig. 5) and, apparently, conditions are created in the 0÷0.8 m section for aggregation of aerosol particles where addition of one element to another is the dominant mechanism. As a result, aerosol moves in the quasi-potential section of the tube (II-III-B section), near the walls of the device in the boundary layer or in a layer close to it.

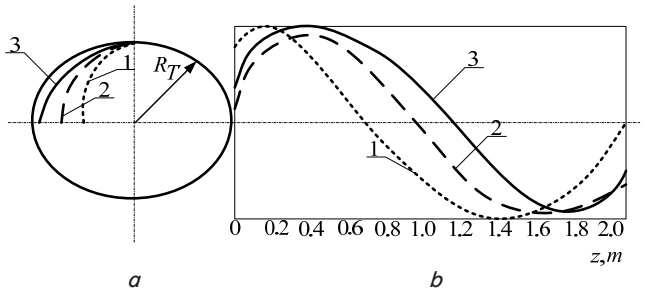

Fig. 6. Trajectory of the aerosol movement along the radius (*a*) and the length (*b*) of the vortex tube: 1 – 0.5 R; 1 – 0.7 R; 1 – 0.9 R; R_T=D_T/2

If aggregation (enlargement) of the aerosol particles actually takes place, then the jumping motion of the rotating aerosol particles and their adjacent vortices must turbulize flow in the layer close to the wall, that is, an effect equivalent to an increase in the Re number should be observed. If the average velocity W_{aver} of the flow remains unchanged in this case, then

$$\Delta P=\rho_T\frac{L}{D_T}\cdot\lambda\cdot W_{cp}^2, \qquad (18)$$

where λ is friction coefficient decreasing with an increase of Re number.

Proceeding from (18), a decrease in resistance with increase in the size of aerosol particles should be expected since only large particles can cause appearance of adjacent vortices. The ash particles will influence mixing of gas particles, the gaseous toxic impurities, their distribution over the volume of the device and kinetics of toxicant conversion. These effects will occur when hydraulic resistance decreases. The ash particles differ in their density from the carrier medium. Thus, at the exit from the vortex tube (B-B section), a layerwise flow is considered with its core of minimum aerosol concentration and the periphery is saturated with aerosol particles. For removal of particles from the volume of the vortex chamber according to Fig. 4, there are a separation tube (5), a forebunker (6) and an aerosol discharge tube (7). These devices should be structurally designed in relation to the concrete operating conditions and concrete vortex tubes.

The energy balance equation (10) together with the equation of radial equilibrium and relationship I=(k/k-1)·(P/ρ) can be written as:

$$\frac{2}{\mathrm{Pr}}\cdot\frac{d}{dr}\cdot\left(r\cdot\frac{di}{dr}\right)=\frac{2}{\mathrm{Pr}}\cdot\frac{\Gamma}{r^2}\cdot\left(\frac{d\Gamma}{dr}-\frac{\Gamma}{r}\right)-r^3\left[d\left(\Gamma/r^2\right)/dr\right]^2-$$
$$-\frac{-rd\left(\Gamma/r^2\right)}{dr}\cdot\left(\frac{d\Gamma}{dr}-\frac{2\Gamma}{r}\right)-\frac{d}{dr}\left(rC_z\frac{dC_z}{dr}\right). \qquad (19)$$

If the radial diagrams of velocities $C\theta(r)$ and $C_z(r)$ are known, then double integration of equation (19) will give a diagram of thermodynamic temperatures.

In the first integration, an arbitrary constant is equal to zero if adiabaticity and conditions of adhesion on the channel wall are taken as boundary conditions. In the second integration, the condition of maintaining total energy along the channel must be met:

$$m_0 i_{00} = 2\pi \int_{r_k}^{R} i_0 \rho C_z r dr, \quad (20)$$

where i_{00} is the enthalpy of braking a flow with mass of $m_0 \rightarrow (Q_0)$ at the entrance to the channel.

To analyze the effect of redistribution of the total energy in the annular channel, the following relationships are used:

$$r = C_1 r^{1-m},$$

$$\frac{d\Gamma}{dr} = C_1 (1-m) r^{-m},$$

where $-1 \le m \le 1$. In this case, relationship between the axial and circumferential component velocities follows from the equation of motion in the following form:

$$rC_z \frac{dC_z}{dr} = \frac{1-m}{m} \cdot \frac{\Gamma}{r} \left(\frac{d\Gamma}{dr} - \frac{\Gamma}{r} \right). \quad (21)$$

The maximum degree of separation of the braking temperature in the annular channel by the swirler relative to ($\theta = 2r/(R-r)$) with flow parameters at the middle diameter at

$$\lambda_{cp} = \sqrt{\frac{C_\theta^2 - C_z^2}{2k/k+1 \cdot R^* T_0}} \text{ and } \beta_{cp} = \arcsin \frac{C_z}{C_\theta}$$

is

$$\overline{\Delta T_0} = \frac{T_{00} - T_{0k}}{T_{00}} =$$

$$= 1 + \left\{ (1-S) \frac{k-1}{k+1} \cdot \frac{\lambda_{cp}^2 \cos^2 \beta_{cp}}{m} \left(\frac{\theta}{\theta - 1} \right)^2 \cdot \left[\left(\frac{\theta - 1}{\theta + 1} \right)^{2m} - 1 \right] \right\}^{-1}, \quad (22)$$

where

$$S = \left(\Pr_T + m(1 + 3\Pr_T) \right) / m;$$

$$\Delta T_{ox} = T_{00} - T_{ox};$$

$$\Delta T_{or} = T_{or} - T_{oo}.$$

Then the amount of heat attributed to the mass of the flowing gas $m_o \rightarrow (Q_o)$ taken from the cold fraction $m_x \rightarrow (Q_1)$ and correspondingly equal to the heat supplied to the hot mass $m_r \rightarrow (Q_3)$ will be:

$$q_x = B \cdot C_p \cdot \Delta T_{OX} = (1-B) \cdot C_p \cdot \Delta T_{O\Gamma}, \quad (23)$$

where

$$B = \frac{m_X}{m_O} \approx \frac{Q_1}{Q_\theta};$$

C_p is the heat capacity of the gas mixture at a constant P.

5. Discussion of the results obtained in studies of the process of scrubbing a gas-dust flow

For the conditions considered in this paper, function $q_x(B)$ has a maximum at $B \approx 0.6$, therefore the range of $0.2 < B < 0.8$ can be taken as the working range of the vortex tube where the temperature separation takes place. Calculations performed at $\rho_T = 1.07$ kg/m^3, $\rho_{aerosol} = 3 \cdot 10^3$ kg/m^3, $k = 1.38$, $T_{00} = 473$ K, $\nu_{gas\ flow} = 2.45 \cdot 10^{-6}$ m^2/s, average molecular mass of the gas flow $\mu = 28.3 \cdot 10^{-3}$ kg/mole, aerosol content $n = 0.20$ g/s, aerosol particle (spherical shape) size $d = 15 \div 40$ μm, gas flow rate 0.8 nm^3/s, $D_T = 0.05$ m allowed us to obtain the ΔT_{OX} dependence on the value of "B" which is shown in Fig. 7.

As is seen in Fig. 7, with growth of aerosol concentration to 0.6 g/s, the cooling effect of flow Q_1 increases and the maxima ΔT_{OX} shift slightly toward smaller "B" values. A further increase in the aerosol concentration leads to pulsating changes of ΔT_{OX} toward lower values. Therefore, the most rational range of "B" values for treatment of the exhaust gas in a vortex tube appears to be within 0.2÷0.5.

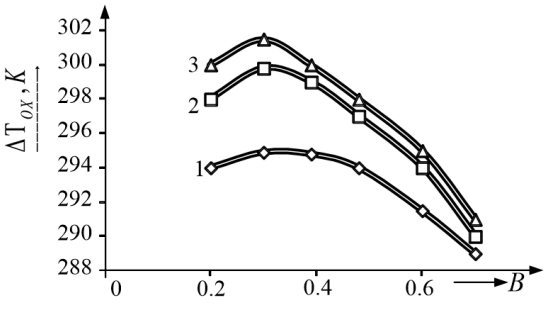

Fig. 7. Efficiency of flow Q_1 cooling in the vortex tube with D_T=0.05 m at various aerosol concentrations in the feed gas flow Q_0: Q_0 without aerosol (1); Q_0 with aerosol concentration of 0.2 g/s (2); Q_0 with aerosol concentration of 0.6 g/s (3)

If "B" parameter for a given flow Q_0 and $\Delta T_{O\Gamma}$ value is known, it is easy to calculate the diaphragm clear section (7) (Fig. 1).

The study results presented in this paper are of practical importance for improving methodology of modeling the process of gas emission scrubbing. The flow of the gas-aerosol stream in the vortex tubes completely agrees with the theory of "rotating (swirling) flows and energy transfer in adiabatic gas flows." It also agrees with the theory of vortex interaction which is used as the basis for explaining physical nature of the energy separation of flows.

The proposed model and methodology can be applied in studies and calculation of systems for scrubbing gas emissions with a simultaneous utilization of exhaust energy of the process gases in various industries (e. g., in soda production or in blast furnaces). The process of preparation of dusty gas streams from the process sources is realized in vortex tubes with a partial recirculation of the heated gas due to the Ranque effect. Calculations showed that the circumferential velocity profile is close to the quasi-solid type of rotation in the region of the swirler, and to the quasi-potential type in the peripheral zone. Namely these phenomena ensure enlargement of dust particles due to their aggregation and creation of thermodynamic conditions for destruction of gaseous toxicants.

6. Conclusions

1. Exhaust gases emitted from process installations contain dust in a concentration of 3 to 15–20 g/Nm^3. Fractional composition of dust is described by a function of multimodal distribution and belongs to a class of fine and very fine dusts with a predominant particle size of less than 15 μm. Specific surface of dust particles is 3 to 10 m^2/g. To ensure effective operation of dust collectors, preliminary preparation of the gas-dust flow is necessary. It changes physico-chemical characteristics of the flow. As the analysis showed, one of the ways to the problem solution is to pretreat the exhaust process gas streams in vortex tubes under conditions ensuring occurrence of the Ranque effect.

2. Axially symmetrical motion of the gas flow with its rotation in the vortex tube was described by the system of Navier-Stokes equations, equations of continuity, energy and gas state using an empirical relationship between viscosity and temperature coefficients. When solving a system of equations, relationship between the turbulent stress tensor and the averaged velocity values (Prantl's hypothesis) in a system of cylindrical coordinates was used. The calculated values of velocity components along the length of the vortex tube were obtained and zones of quasi-solid and quasi-potential rotation of the dust flow were determined. Trajectories of aerosol motion along the tube radius and length were determined. It was established that at the exit from the tube, aerosol moves as a dense layer near the inner walls and the dust-free gas stream moves by the tube axis. It was also established that conditions were created for the occurrence of the Ranque effect and temperatures brake when Re≥10^5.

3. Based on the analysis of the developed calculation model, obtained solutions and thermodynamic and kinetic calculations, it was shown that a thermal separation takes place in the zone of quasi-solid flow rotation in the vortex tube at Re≥105. At temperatures ≥673 K, thermodynamic conditions are created for destruction of NO_x, SO_x, CO in the presence of water vapor. Due to high velocities of collision of dust particles, agglomeration processes occur in the zone of quasi-solid flow rotation with a fivefold or sixfold increase in the particle size.

Thus, the main conclusion is that the preliminary treatment of the dust-gas flow in the vortex tubes will increase efficiency of the dust collectors and ensure overall purification of exhaust gases.

References

1. Chekalova, L. V. Ekotekhnika. Zashchita atmosfernogo vozduha ot vybrosov pyli, aerozoley i tumanov [Text] / L. V. Chekalova. – Yaroslavl': Rus', 2004. – 424 p.
2. Zaytsev, O. N. Issledovanie protsessov lokalizatsii teplovyh vybrosov zakruchennymi potokami [Text] / O. N. Zaytsev // Ekotekhnologiya i resursosberezhenie. – 2002. – Issue 6. – P. 70–72.
3. Pat. No. 2430971 RU. Sposob suhoy ochistki domennogo gaza. MPK C21B 7/22 [Text] / Osipenko V. V., Osipenko V. D. – No. 2009132782/02; declareted: 31.08.2009; published: 10.10.2011, Bul. No. 28.
4. Pat. No. 2415718 RU. Tsiklon s vhodnym patrubkom-separatorom i obvodnymi trubami dlya otvoda melkih chastits. MPK B04 C5/02 (2006.01), B04 C5/12 (2006.01), C21 B7/22 (2006.01) [Text] / Evans P., Federston U. B. – No. 2009134521/05; declareted: 13.02.2008; published: 10.04.2011, Bul. No. 10.
5. Grunewald, G. Initial soil development in alkaline waste of soda production [Text] / G. Grunewald. – Der Andere Verlag, 2010. – 119 p.
6. Richard, O. M. Environmental engineering: principles and practice [Text] / O. M. Richard. – Wiley-Blackwell, 2014. – 662 p.
7. Vetoshin, A. G. Inzhenernaya zashchita okruzhayushchey sredy ot vrednyh vybrosov [Text]: ucheb. pos. / A. G. Vetoshin. – 2-e izd. ispr. i dop. – Moscow: Infra-Inzheneriya, 2016. – 416 p.
8. Zlygostev, A. S. Metody ochistki i obezvrezhivaniya ventilyatsionnyh i tekhnologicheskih vybrosov [Electronic resource] / A. S. Zlygostev // Zelenaya planeta. – Available at: http://ecologylib.ru
9. Hitrova, I. V. Tekhnologiya utilizatsyi gazovyh vybrosov, tverdyh othodov i shlakov [Text] / I. V. Hitrova, T. B. Novozhilova. – Kharkiv: NTU «KhPI», 2004. – 218 p.
10. Grivko, E. V. Otsenka stepeni antropogennoy preobrazovannosti prirodno-tekhnogennyh sistem [Text]: ucheb. pos. / E. V. Grivko, O. S. Ishanova. – Orenburg: OOO IPK «Universitet», 2013. – 128 p.
11. Amirov, R. Ya. Tekhnologicheskie sistemy: Protsessy, konstruktsii, effektivnost' [Text] / R. Ya. Amirov, I. M. Urakaev, R. G. Gareev. – Ufa: Gilem, 2000. – 600 p.
12. Batluk, V. A. Zalezhnist efektyvnosti pylovlovlennia vidtsentrovoinertsiynykh aparativ vid konstruktsyi bunkera [Text] / V. A. Batluk, O. V. Melnikov, O. V. Mirus // Promyslova hidravlika i pnevmatyka. – 2011. – Issue 2 (32). – P. 44–47.
13. Shaporev, V. P. Deiaki aspekty modeliuvannia prystroiu kontaktuvannia faz [Text] / V. P. Shaporev, M. I. Vasyliev // Promyslova hidravlika i pnevmatyka. – 2011. – Issue 2 (32). – P. 41–43.
14. Kutepov, A. M. Vihrevye protsessy dlya modifikatsyi dispersnih sistem [Text] / A. M. Kutepov, A. S. Latkin. – Moscow: Nauka, 1999. – 270 p.
15. Bogomolov, A. On Inertial Systems, Dust Cleaning and Dust Removal Equipment, and Work Areas in the Production of Aerated Concrete from the Hopper Suction Apparatus CSF [Text] / A. Bogomolov, N. Sergina, T. Kondratenko // Procedia Engineering. – 2016. – Vol. 150. – P. 2036–2041. doi: 10.1016/j.proeng.2016.07.290
16. Chelnokov, A. A. Inzhenernye metody ohrany atmosfernogo vozduha [Text] / A. A. Chelnokov, A. F. Mironchik, I. N. Zhmyhov. – Minsk: Vysheyshaya shkola, 2016. – 397 p.
17. Thakare, H. R. Experimental, computational and optimization studies of temperature separation and flow physics of vortex tube: A review [Text] / H. R. Thakare, A. Monde, A. D. Parekh // Renewable and Sustainable Energy Reviews. – 2015. – Vol. 52. – P. 1043–1071. doi: 10.1016/j.energy.2015.03.058

18. Volkov, K. N. Metody uskoreniya gazodinamicheskih raschetov na nestrukturirovannyh setkah [Text] / K. N. Volkov, Yu. N. Deryugin, V. N. Emel'yanov, A. G. Karpenko, A. S. Kozelkov, I. V. Teterina. – Moscow: FIZMATLIT, 2014. – 536 p.
19. Landau, L. D. Teoreticheskaya fizika. Vol. I [Text]: ucheb. pos. / L. D. Landau, E. M. Lifshits. – 5-e izd. – Moscow: «FIZMATLIT», 2013. – 224 p.
20. Molochko, F. I. O sushchnosti vihrevogo effekta Ranka-Hil'sha [Text] / F. I. Molochko // Problemy obshchey energetiki. – 2015. – Issue 4 (43). – P. 58–60.
21. Yahno, O. M. Gidrodinamicheskiy nachal'nyy uchastok [Text] / O. M. Yahno, V. M. Matiega, V. S. Krivosheev. – Chernovtsy, 2004. – 145 p.
22. Zuykov, A. L. Gidravlicheskoe modelirovanie kontrvihrevyh techeniy [Text] / A. L. Zuykov // Vestnik MGSU. – 2014. – Issue 6. – P. 114–125.
23. Akhmetov, D. G. Swirl flow in vortex chamber [Text] / D. G. Akhmetov, T. D. Akhmetov // Science Bulletin. – 2015. – Vol. 6, Issue 4. – P. 109–120. doi: 10.17117/nv.2015.04.109
24. Frumin, V. M. Sposoby suhoy ochistki gaza kal'tsinatsyi ot sodovoy pyli [Text] / V. M. Frumin, V. M. Gut, V. L. Burin et. al. // Himiya i tekhnologiya osnovnoy himicheskoy promyshlennosti. – 2016. – Vol. 78. – P. 52 57.
25. Gutsol, A. F. The Ranque effect [Text] / A. F. Gutsol // Uspekhi Fizicheskih Nauk. 1997. – Vol. 167, Issue 6. – P. 665–687. doi: 10.3367/ufnr.0167.199706e.0665
26. Shaporev, V. P. To a question about the nature of the relationship of water to calcium hydroxide [Text] / V. P. Shaporev, I. V. Pitak, M. I. Vasil'ev // Visnyk NTU «KhPI». – 2015. – Issue 50 (1159). – P. 121–127.
27. Shaporev, V. P. Priblizhennoe reshenie uravneniya koagulyatsyi s nekotorymi model'nymi yadrami [Text] / V. P. Shaporev, M. D. Kogut // Ekologiya himicheskoy tekhniki i biotekhnologyi. – 1996. – Vol. 2. P. 73–77.
28. Pitak, I. V. Study of experimental-industrial design of rotary vortex machine [Text] / I. V. Pitak // Technology audit and production reserves. – 2014. – Vol. 3, Issue 2 (17). – P. 33–38. doi: 10.15587/2312-8372.2014.26212
29. Kolyadin, E. A. Vliyanie zakrutki potoka gazov na konvektivnyi teploobmen v utilizatsionnyh gazotrubnyh kotlah [Text] / E. A. Kolyadin // Vestnik Astrahanskogo gosudarstvennogo tekhnicheskogo universiteta. – 2007. – Issue 2 (37). – P. 159–162.
30. Bona, C. Elements of Numerical Relativity and Relativistic Hydrodynamics [Text] / C. Bona, C. Palenzuela-Luque, C. Bona-Casas // Lecture Notes in Physics. – 2009. doi: 10.1007/978-3-642-01164-1
31. Konovalov, V. I. Sushka i drugie tekhnologicheskie protsessy s vihrevoy trubkoy Ranka-Hil'sha: vozmozhnosti i eksperimental'naya tekhnika [Text] / V. I. Konovalov, A. Yu. Orlov, N. T. Gatapova // Estnik TGTU. – 2010. – Vol. 16, Issue 4. – P. 803–825.
32. Bochkarev, V. V. Optimizatsiya himiko-tekhnologicheskih protsessov [Text]: ucheb. pos. / V. V. Bochkarev. – Moscow: Yurayt, 2016. – 263 p.
33. Korkodinov, Ya. A. Primenenie effekta Ranka-Hil'sha [Text] / Ya. A. Korkodinov, O. G. Hurmatullin // Vestnik Permskogo natsional'nogo issledovatel'skogo universiteta. – 2012. – Issue 4. – P. 42–53.
34. Protopopov, R. Ya. About reactor modeling for organic impurities thermal neutralization [Text] / R. Ya. Protopopov, O. N. Filenko, V. P. Shaporev // Eastern-European Journal of Enterprise Technologies. – 2012. – Vol. 2, Issue 12 (56). – P. 22–26. – Available at: http://journals.uran.ua/eejet/article/view/3925/3593
35. Protopopov, R. Ya. Analiz termichnoho metodu zneshkodzhennia hazovykh vykydiv vid orhanichnykh spoluk [Text] / R. Ya. Protopopov // Inovatsiini shliakhy modeliuvannia bazovykh haluzei promyslovosti, enerho- ta resursozberezhennia, okhorona navkolyshnoho seredovyshcha. – Kharkiv: UkrHNTTs «Enerhostal», 2012. P. 379–386.
36. Tovazhnyans'kiy, L. L. Teploenergetika pogruzhnogo goreniya v reshenyi problem teplosnabzheniya i ekologyi Ukrainy [Text] / L. L. Tovazhnyans'kiy, L. P. Pertsev, V. P. Shaporev // Intehrovani tekhnolohii ta enerhozberezhennia. – 2004. – Issue 3. – P. 3–12.